

Structural Changes of Water in the Schiff Base Region of Bacteriorhodopsin: Proposal of a Hydration Switch Model[†]

Taro Tanimoto, Yuji Furutani, and Hideki Kandori*

Department of Applied Chemistry, Nagoya Institute of Technology, Showa-ku, Nagoya 466-8555, Japan

Received October 11, 2002; Revised Manuscript Received January 6, 2003

ABSTRACT: In a light-driven proton-pump protein, bacteriorhodopsin (BR), three water molecules participate in a pentagonal cluster that stabilizes an electric quadrupole buried inside the protein. In low-temperature Fourier transform infrared (FTIR) K minus BR spectra, the frequencies of water bands suggest extremely strong hydrogen bonding conditions in BR. The three observed water O–D stretches, at 2323, 2292, and 2171 cm^{-1} , are probably associated with water that interacts with the negative charges in the Schiff base region. Retinal isomerization weakens these hydrogen bonds in the K intermediate, but not in the later intermediates such as L, M, and N. In these states, spectral changes of water bands appeared only in the $>2500 \text{ cm}^{-1}$ region, which correspond to weak hydrogen bonds. This observation suggests that after the K state the water molecules in the Schiff base region find a hydrogen bonding acceptor. We propose here a model for the mechanism of proton transfer from the Schiff base to Asp85. In the “hydration switch model”, hydration of a water molecule is switched in the M intermediate from Asp85 to Asp212. This will have increased the pK_a of the proton acceptor, and the proton transfer is from the Schiff base to Asp85. The present results also suggest that the deprotonated Asp96 in the N intermediate is stabilized in a manner different from that of Asp85 in BR.

Proteins that actively pump protons across membranes must translocate them through hydrophobic regions inside the protein. Therefore, internal water molecules are presumed to play a crucial role in active proton transport (1, 2). The water may participate in hydrogen bonding networks inside proteins that constitute proton pathways, and in the switch reaction by mediating an essential proton transfer at the active site (2). While little is generally known about the structure and function of internal water molecules in such proteins, the greatest progress has been made in bacteriorhodopsin (BR).¹

BR is a light-driven proton pump in *Halobacterium salinarum* that contains *all-trans*-retinal as a chromophore (3, 4). The retinal binds to Lys216 through the protonated Schiff base linkage ($\text{C}=\text{NH}^+$), and there are two positive (Schiff base and Arg82) and two negative (Asp85 and Asp212) charges in the Schiff base region (Figure 1). The crystallographic structure of BR showed that three water molecules constitute a pentagonal cluster structure, which must stabilize the electric quadrupole at the Schiff base (5, 6). Upon absorption of light, photoisomerization takes place from the *all-trans* to the 13-*cis* form in sub-picoseconds, followed by the primary proton transfer from the Schiff base to Asp85 in tens of microseconds. It is generally accepted that the proton transfer that occurs in the transition from the

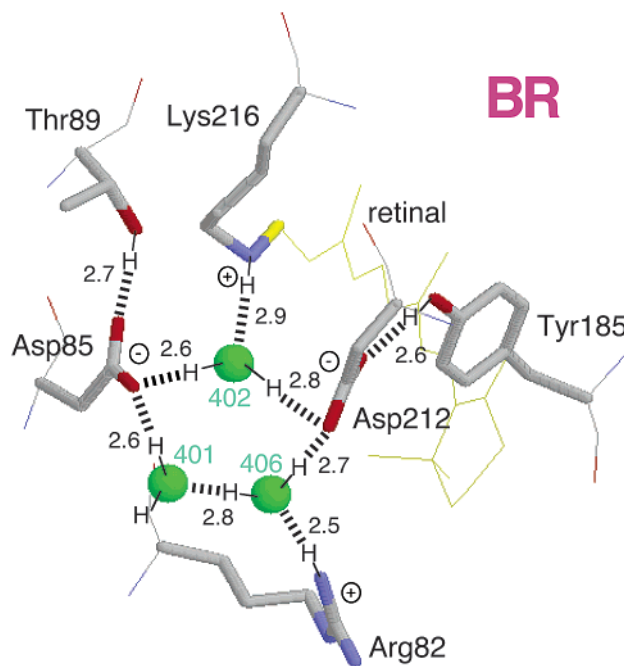


FIGURE 1: X-ray crystallographic structures of the Schiff base region in BR from PDB entry 1C3W (5). The membrane normal is approximately in the vertical direction of this figure. Top and bottom regions correspond to the cytoplasmic and extracellular sides, respectively. Green spheres (water401, -402, and -406) represent water molecules which form a roughly pentagonal cluster with an oxygen from Asp85 and an oxygen from Asp212. The water-containing pentagonal cluster structure will stabilize an electric quadrupole in this region. Hydrogen atoms and hydrogen bonds (dashed lines) are deduced from the structure, while the numbers are the hydrogen bonding distances in angstroms.

[†] This work was supported by Grants 14380316, 14045238, and 13024242 from the Japanese Ministry of Education, Culture, Sports, Science, and Technology to H.K.

* To whom correspondence should be addressed. Phone and fax: 81-52-735-5207. E-mail: kandori@ach.nitech.ac.jp.

¹ Abbreviations: BR, bacteriorhodopsin; FTIR, Fourier transform infrared; HR, halorhodopsin.

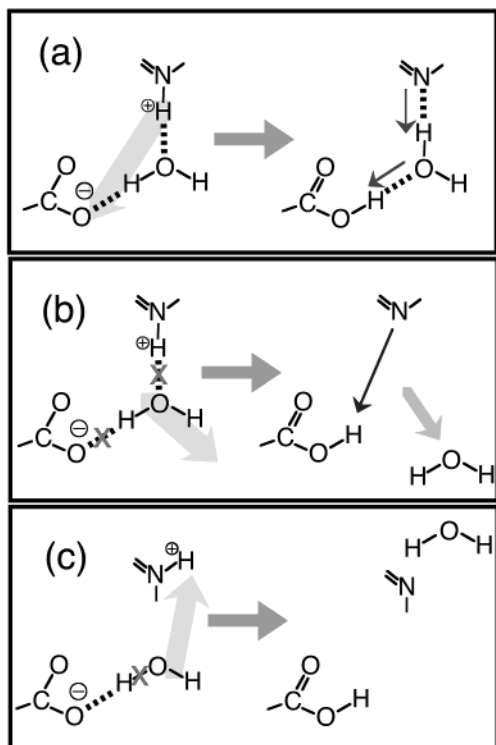


FIGURE 2: Schematic drawing of the water-mediated proton transfer in the Schiff base region of BR. (a) Proton transfer through the bridged water molecules in a coherent manner. In this model, the specific geometry of the hydrogen bonding network in L allows proton transfer from the Schiff base to Asp85. (b) In this model, the bridged water molecule is pulled out of the hydrogen bond so that the difference in the pK_a values becomes sufficiently small to jump a proton from the Schiff base to Asp85 directly. (c) Hydroxide transfer model. In this model, the “proton pump” is actually a hydroxide (OH^-) pump, the bridged water is dissociated into a proton and a hydroxide, and hydroxide moves from the extracellular to the cytoplasmic domain.

L to the M intermediate ensures the directionality in the pump, because the accessibility is switched from the extracellular side to the cytoplasmic side, upon either the formation of M or the early-to-late M transition (3, 4).

The mechanism of the proton transfer from the Schiff base to Asp85 has therefore attracted much interest. The water molecules in the Schiff base region presumably play important roles in the proton transfer reaction (2). How do these waters change during the BR function? With regard to the mechanism of proton transfer, three models have so far been taken into account (2). Figure 2 illustrates schematic drawings of the models, where both pretransfer (L intermediate) and posttransfer (M intermediate) states are given. In the first model, a water molecule acts as the direct mediator of the proton transfer from the Schiff base to Asp85 (Figure 2a). The proton is transferred concertedly through the proton wire. In the second model, a water is not involved in the proton transfer. On the contrary, its motion out of its original bridging position controls the pK_a of the donor and acceptor (Figure 2b). The third model argues that “proton transfer” is in fact hydroxide transfer, not proton transfer (7). According to this model, a hydroxide (OH^-) moves from the extracellular to the cytoplasmic domain as does a chloride ion in the D85T mutant BR (Figure 2c) (8).

As shown by these models, a key issue is the change in the interaction of the water molecules in the Schiff base

region (Figure 1). This information must be strongly related to the mechanism of proton transfer reactions. The recent crystallographic structures of photocycle intermediates of BR have reported the location of internal water molecules in K (9, 10), L (11), and M (12–16). Another useful tool in the study of internal water molecules is low-temperature Fourier transform infrared (FTIR) spectroscopy. Although the frequency region was limited to the water bands under weak hydrogen bonds in the previous FTIR spectroscopy (17–30), we have demonstrated the possibility of detecting the stretching vibration of water molecules associating with negative charges (31, 32). The spectral analysis of the K minus BR spectra in D_2O and D_2^{18}O indeed revealed the presence of the water stretching vibrations under very strong hydrogen bonding conditions, which was interpreted in terms of water molecules associating with negative charges (32). The quantum mechanical and molecular mechanical (QM/MM) calculation of the Schiff base region in BR by Hayashi and Ohmine (33) showed that the water O–D stretch at the lowest frequency (2171 cm^{-1}) corresponds to the stretching mode of water402 bound to Asp85. Upon formation of K, the extremely strong interaction between water402 and Asp85 is weakened as shown by a shift to a higher frequency. The rotational motion of water402 was also suggested by the polarized measurements (32).

Since the IR observations of the O–D stretch of water in all the stretching vibrational frequencies provided new information about the water structural changes before and after retinal isomerization (32), their extension study for late photointermediates will lead to better understanding of water structural changes during the proton pumping of BR. In this article, we report the IR difference spectra in the water O–D stretching region of the K, L, M, and N photointermediates. In contrast to the K minus BR spectrum, we did not observe spectral changes of water bands under strong hydrogen bonding conditions in the difference spectra for late intermediates such as L, M, and N. On this basis, we propose here a model for the mechanism of proton transfer from the Schiff base to Asp85. In the model we call the “hydration switch model”, hydration of a water is switched from Asp85 in the L intermediate to Asp212 in the M intermediate, which increases the pK_a of the proton acceptor, and a proton transfer from the Schiff base to Asp85 takes place.

MATERIALS AND METHODS

Samples were prepared as described previously (31, 32). A $120\text{ }\mu\text{L}$ aliquot of the sample in 2 mM phosphate buffer (pH 7) or 2 mM borate buffer (pH 10), for the K minus BR and L minus BR spectra or the M minus BR and N minus BR spectra, respectively, was dried on a BaF_2 window with diameter of 18 mm . After hydration by $1\text{ }\mu\text{L}$ of D_2O or D_2^{18}O , the sample was placed in a cell, and then the cell was mounted in an Oxford DN-1704 cryostat. The film was illuminated with $>500\text{ nm}$ light for 1 min at 273 K to obtain the light-adapted state of BR.

Polarized infrared spectroscopy was applied as described previously by use of a Bio-Rad FTS-40 FTIR spectrometer (31, 32, 34, 35). One change was made for the present equipment. CO_2 gas in the dry air supplied to the spectrometer was not removed in the previous experimental setup, which resulted in noisy spectra in the $2400\text{--}2300\text{ cm}^{-1}$

region (31, 32). We removed CO₂ gas by using an additional filter in these measurements, which provides less noisy signals in the 2400–2300 cm⁻¹ region. We re-recorded the K minus BR spectra using this setup.

The L minus BR and M minus BR spectra were obtained with 2 cm⁻¹ resolution as described previously (21, 24, 27, 36). Illumination with >600 nm light at 170 K for 1 min converted BR to the L intermediate. On the other hand, illumination with >500 nm light at 230 K for 1 min converted BR to the M intermediate. Since the M intermediate reverted to BR upon illumination with 420 nm light (by using an interference filter) for 2 min, as evidenced by the same but inverted spectral shape, cycles of alternating illumination with >500 nm light and 420 nm light were repeated a number of times. For the L minus BR and M minus BR spectra, 5 and 16 independent measurements were averaged with 128 scans, respectively.

The N minus BR spectra were obtained with 2 cm⁻¹ resolution as described previously (28, 37). Illumination with >500 nm light at 273 K for 30 s converted BR to the N intermediate. Since the N intermediate completely reverted to BR in 8 min at 273 K, we were able to repeat the measurements for signal averaging. There were spectral changes without illumination in the 2800–1900 cm⁻¹ region (for water O–D stretches) at 273 K, so we recorded the difference (called “baseline”) between the two spectra without intermittent illumination and subtracted it from the data when necessary. We averaged 25 independent measurements with 32 scans. The M intermediate was also contained under these conditions. We estimated the contents of the M and N intermediates from the analysis of the positive 1186 cm⁻¹ band, which probes the C–C stretch of the protonated 13-*cis*-retinal only present in the N intermediate.

RESULTS

Figure 3 shows the K minus BR (a), L minus BR (b), M minus BR (c), and N minus BR (d) spectra recorded at 77, 170, 230, and 273 K, respectively. These spectra were normalized for the negative 1202 cm⁻¹ band, indicating that the same number of BR molecules are converted to intermediates. It is noted that Figure 3d contains also an M minus BR spectral component. From the analysis of the positive 1186 cm⁻¹ band that probes the C–C stretch of the protonated 13-*cis*-retinal, we estimated the photoproduct to be 70% N and 30% M. In our previous FTIR measurements in H₂O, the composition was estimated to be 85% N and 15% M (37). The lower content of the N intermediate in the study presented here originates from intentionally lower-level hydration in D₂O intended to increase the signal-to-noise ratio in the 2700–1900 cm⁻¹ region. We confirmed that the current N minus BR spectrum is identical in the 1800–900 cm⁻¹ region to that under fully hydrated conditions (data not shown).

Water Stretching Vibrations in the K minus BR Spectra. Figure 3a shows the K minus BR spectra. Since the signal-to-noise ratio in the frequency region of CO₂ gas (2400–2300 cm⁻¹) becomes better, we observed new IR bands there. We previously reported that there are peaks at 2359 (+), 2292 (–), 2265 (+), 2171 (–), and 2123 (–) cm⁻¹ in the 2400–2000 cm⁻¹ region (31, 32). There are additional bands at 2406 (–), 2391 (+), and 2323 (–) cm⁻¹ (Figure 3a). The

bands at 2359 (+), 2323 (–), 2292 (–), 2265 (+), and 2171 (–) cm⁻¹ exhibited the isotope shift of water, indicating that such spectral changes contain water O–D stretches. It is noted that the 2323, 2292, and 2171 cm⁻¹ bands of BR correspond to the water O–H stretches in the 3100–2800 cm⁻¹ region, which are much lower in frequency than those of the fully hydrated tetrahedral water molecules (3540 and 3240 cm⁻¹) (32, 38). Therefore, we concluded that the water molecules associate with negative charges in the Schiff base region (Figure 1) (32). It is particularly noted that the water O–D stretch at 2171 cm⁻¹ is extremely low, suggesting that the hydrogen bond of the water is extremely strong. Hayashi and Ohmine reported on the basis of their QM/MM calculations (33) that the 2171 cm⁻¹ band corresponds to the O–D stretch of water₄₀₂ being hydrogen bonded with Asp85 (2.6 Å, Figure 1).

Upon formation of K, it seems that these water O–D stretches shift to higher frequencies, indicating that the hydrogen bonds are weakened. Retinal motion in the restricted protein environment yields perturbation of the hydrogen bonding network in the Schiff base region, which probably weakens the association of the water with negative charges. In fact, we observed rotation of a water molecule by means of polarized FTIR spectroscopy (32).

Figure 3a shows that most bands in the 2700–2000 cm⁻¹ region originate from water O–D stretches. On the other hand, some other bands have already been identified. We assigned the 2506 (–)/2466 (+) cm⁻¹ bands as the O–D stretch of Thr89 by using a [3-¹⁸O]threonine-labeled BR sample (34). A low frequency (2506 cm⁻¹) as the threonine O–D stretch in BR is an indication of a strong hydrogen bond of Thr89, which is consistent with the BR structure (Figure 1). A lower-frequency shift to 2466 cm⁻¹ in K implies a further strengthened hydrogen bond of Thr89, presumably with Asp85. This observation was not consistent with the K structure by Edman et al. (9), since they described the interaction between Thr89 and Asp85 as being broken. In contrast, it is consistent with the K structure by Schobert et al. (10). We assigned the negative 2171 and 2123 cm⁻¹ bands to the N–D stretch of the Schiff base by using a [ζ -¹⁵N]lysine-labeled BR sample (39). The presence of the N–D stretch of the Schiff base at the same frequency as the O–D stretch of water is one of the reasons for small isotope shift of water for the 2171 cm⁻¹ band (Figure 3a). The N–D stretch of the Schiff base appears at ~2466 cm⁻¹ in the K intermediate, indicating that the hydrogen bond of the Schiff base is significantly weakened. This view is supported by the recent X-ray structure of the K intermediate (10). Polarized measurements suggested that the N–D group of the Schiff base in K is oriented along the membrane (39). Thus, Figure 3a exhibits strong perturbation of the Schiff base region (Figure 1) upon retinal photoisomerization through the analysis of stretching vibrations. Since the X–D stretching vibrations are direct probes of hydrogen bonds, we expected to gain information about the hydrogen bonding alterations in late intermediates, particularly on the water molecules.

Water Stretching Vibrations in the L minus BR Spectra. Figure 3b shows the L minus BR difference spectra measured at 170 K and pH 7. Unlike the K minus BR spectra, the L minus BR difference spectra did not exhibit an isotope effect of water in the <2500 cm⁻¹ region. This fact implies that

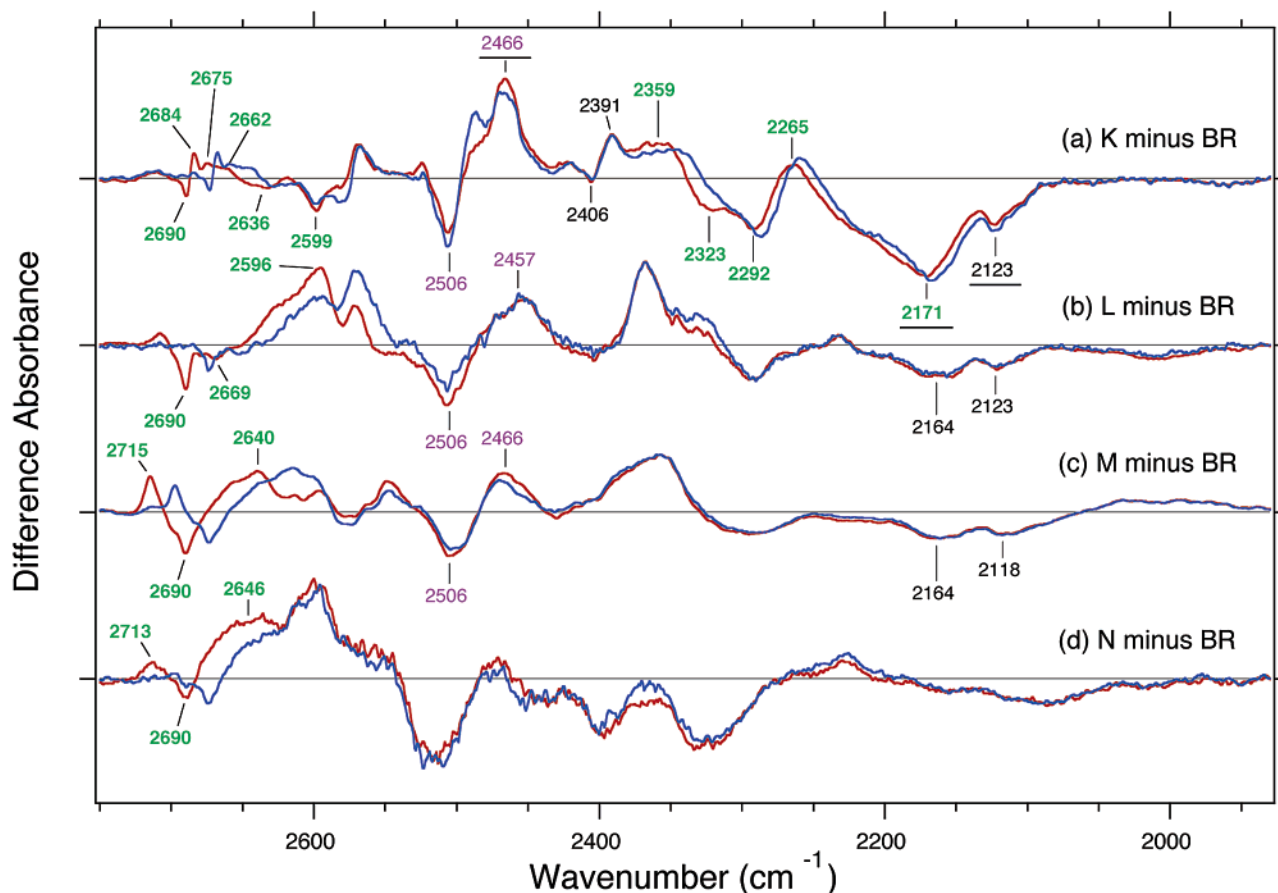


FIGURE 3: Difference IR spectra are compared between hydration with D_2O (red lines) and $D_2^{18}O$ (blue lines) in the 2750–1930 cm^{-1} region. The window tilting angle is 53.5° in the polarized IR measurements. The K minus BR (a), L minus BR (b), M minus BR (c), and N minus BR (d) spectra are measured at 77, 170, 230, and 273 K, respectively, where 24, 5, 16, and 25 independent measurements with 128, 128, 128, and 32 scans were averaged, respectively. These spectra are normalized at the negative 1202 cm^{-1} band, indicating that the same numbers of BR molecules are converted to intermediates. One division of the y-axis corresponds to 0.0025 absorbance unit. Green-labeled frequencies correspond to those identified as water stretching vibrations. Purple-labeled frequencies are O–D stretches of Thr89 (34, 36), while the underlined frequencies are N–D stretches of the Schiff base (39).

the water molecules in the Schiff base region re-form strong hydrogen bonds with the negative charge(s). The L minus BR spectrum exhibits negative water bands at 2690 and 2669 cm^{-1} , while broad positive feature due to water appeared in the 2650–2560 cm^{-1} region (Figure 3b). The analysis of these water bands was reported for the O–H stretching region (2, 17, 18, 20, 21, 23). By using mutants, the water molecules having stretches at 2690 or 2669 cm^{-1} were estimated to be near Asp85 (18) or the cytoplasmic region (21, 23), respectively.

It is an intriguing contrast that both 2690 and 2171 cm^{-1} bands correspond to the water stretching vibrations in the Schiff base region, whose frequencies differ by $>500\text{ }cm^{-1}$ ($>800\text{ }cm^{-1}$ as the O–H stretch). The former is free from hydrogen bonds, while the latter is under extremely strong hydrogen bonding conditions. The previous QM/MM calculations assigned 2690 and 2171 cm^{-1} bands as the O–D stretch of water401 without a hydrogen bond and the O–D stretch of water402 being hydrogen-bonded with Asp85, respectively (Figure 1) (33). The L intermediate has water stretching vibrational modes different from those of BR only for the weakly hydrogen bonded waters, and strongly hydrogen bonded waters of L are identical in vibrational character to those of BR (Figure 3b). In other words, the re-establishment of the interaction of water molecules with

negative charges may be an important element in the K-to-L transition.

It is noted that there are spectral changes in the 2400–2000 cm^{-1} region for the strongly hydrogen bonded waters, though they do not originate from water O–D stretches. In particular, a strong negative feature of the K minus BR spectrum in the 2250–2050 cm^{-1} region is severely reduced in magnitude in the L minus BR spectrum. The two remaining negative bands at 2164 and 2123 cm^{-1} are close in frequency to the N–D stretch of the Schiff base. The assignment of these bands is in progress.

Water Stretching Vibrations in the M minus BR Spectra. Figure 3c shows the M minus BR difference spectra measured at 230 K and pH 10. We expected some IR spectral changes of the strongly hydrogen bonded water in the Schiff base region, because proton transfer from the Schiff base to Asp85 in the M intermediate takes place. Nevertheless, no isotope effect of water molecules was observed in the $<2500\text{ }cm^{-1}$ region. As for the case of the L minus BR spectra, only an isotope shift of water was observed in the $>2600\text{ }cm^{-1}$ region. The analysis of the water bands at 2715 (+), 2690 (–), and 2640 (+) cm^{-1} was reported for the O–H stretching region (2, 17, 22, 24, 27, 28). The origin of the negative 2690 cm^{-1} band is the same as in the L minus BR spectrum, being from a water near Asp85 (2). By using

mutants, the water molecules having stretches at 2715 or 2640 cm^{-1} were suggested to be at the cytoplasmic region (2, 28, 30). Figure 3c shows the measurements at pH 10, while the same result, i.e., no isotope effect of water molecules in the $<2500 \text{ cm}^{-1}$ region, was obtained for the measurements at pH 7 (data not shown).

The lack of isotope shifts of water in the lower-frequency region indicates that the strongly hydrogen bonded waters of M are identical in their vibrational characteristics to those of BR. If the 2171 cm^{-1} band originates from the O–D stretch of water402 being hydrogen bonded with Asp85, as shown by Hayashi and Ohmine (33), the hydrogen bond between water402 and Asp85 would not be as strong in the M intermediate because of the disappearance of a negative charge at position 85. This requires formation of an extremely strong hydrogen bond from another interaction inside BR. We will propose a model of the proton transfer from the Schiff base to Asp85 based on this fact.

The M minus BR spectrum exhibits negative bands at 2164 and 2118 cm^{-1} , which are similar to those for the L minus BR spectrum. As mentioned, they could originate from the N–D stretch of the Schiff base in BR, which disappears in M because of deprotonation. There are also bands at 2506 (+) and 2466 (–) cm^{-1} , whose spectral features look similar to those of the L minus BR spectrum. They were previously assigned as the O–D stretch of Thr89 (36).

Water Stretching Vibrations in the N minus BR Spectra. A proton is transferred from Asp96 in the cytoplasmic side to the Schiff base, accompanying the M-to-N transition. The distance between Asp96 and the Schiff base is $>11 \text{ \AA}$ in M (12–16), and internal water molecules must assist the proton transfer. In addition, Asp96 is deprotonated in N, indicating that a negative charge newly appears at the hydrophobic cytoplasmic domain. These facts may suggest some IR spectral changes in the strongly hydrogen bonded water at the cytoplasmic region. Figure 3d shows the N minus BR difference spectra measured at 273 K, which also contains the 30% M minus BR spectrum. As for L and M, no isotope shift of water molecules was observed in the $<2500 \text{ cm}^{-1}$ region. We reported the analysis of the water bands at 2713 (+), 2690 (–), and 2646 (+) cm^{-1} previously for the O–H stretching region (2, 28). The origin of the negative 2690 cm^{-1} band is a water near Asp85 (2). By using mutants, the water having stretches at 2713 or 2646 cm^{-1} were suggested to be at the cytoplasmic region (2, 28).

The lack of isotope shifts of water in the lower-frequency region indicates that the strongly hydrogen bonded waters of N are identical in vibrational character to those of BR and M. This result also suggests that there is no strong association of water molecules with negatively charged Asp96 in N, unlike the case of Asp85 in BR.

DISCUSSION

In this article, we report water structural changes during the photocycle of BR. In the earlier FTIR spectroscopic studies (17–30), the frequency region was limited to water bands with weak hydrogen bonds, but now we could extend the frequency region to cover all of the water stretching vibrations. Consequently, we detected water bands under extremely strong hydrogen bonding conditions in the K minus BR spectrum. Three water O–D stretches of BR at 2323, 2292, and 2171 cm^{-1} correspond to those under strong

hydrogen bonding conditions, which originates presumably from association with the negative charges in the Schiff base region (Figure 1). Among them, the band at 2171 cm^{-1} is extremely low as the water O–D stretch, and the QM/MM calculation of the Schiff base region in BR showed that the band corresponds to the stretching mode of water402 bound to Asp85 (33).

Unlike in K, we did not observe spectral changes of the water bands under strong hydrogen bonding conditions in L, M, and N (Figure 3). Spectral changes of water bands appeared only in the $>2500 \text{ cm}^{-1}$ region, which are for weak hydrogen bonds. These results were unexpected, but we need to interpret them in terms of water structural changes. Below, we propose a model of the proton transfer from the Schiff base to Asp85 on the basis of these IR observations.

In the unphotolyzed state of BR, the position of water402 appears to be symmetrical with respect to Asp85 and Asp212 (Figure 1). However, a stronger interaction between water402 and Asp85 was suggested by the QM/MM calculation of the Schiff base region (33). This may be consistent with the fact that the pK_a of the Schiff base is more influenced by the mutation of Asp85 than that of Asp212 (40). Thus, it is likely that the O–D stretch of water402 bound to Asp85 is at 2171 cm^{-1} (Figure 4). Upon photoisomerization, the N–D group of the Schiff base is displaced to a parallel orientation to the membrane (39). As a consequence, the water-containing pentagonal cluster structure is perturbed, and the interaction between water402 and Asp85 is weakened (Figure 4). Such structural change possibly involves rotational motion of water402 (32). These FTIR results are consistent with the recent structural (10) and theoretical (41) studies for the K intermediate.

The water band of BR at 2171 cm^{-1} is changed in K, whereas the band is restored in L, M, and N (Figure 3). Since the frequency (2171 cm^{-1}) is extremely low for a water stretch, we postulate that the hydrogen-bonding acceptor of the water is negatively charged. This means that it would be either Asp85 or Asp212 in L, and Asp212 in M. We propose here that water402 forms a strong hydrogen bond (i) with Asp85 in L and (ii) with Asp212 in M (Figure 4). The K-to-L transition accompanies relaxation around the retinal chromophore, which involves water structural changes. Reassociation of water402 with Asp85 is one of these changes, which presumably stabilizes the negative charge at position 85 in L. According to our model, then, the hydration switch of water402 takes place from Asp85 to Asp212 so that the M intermediate is formed accompanying proton transfer from the Schiff base to Asp85 (Figure 4). Thus, the simple hydration switch model can explain these IR data and the mechanism of proton transfer in the Schiff base. The hydration state in the Schiff base region would be the same in N as in M.

Our model, the hydration switch model, is closer to the second model of Figure 2, where motion of a water molecule controls the relative pK_a of the proton donor and acceptor. It is noted that our observation does not rule out the other two models at this moment. However, the hydration switch model is simple and straightforward. For instance, we do not have to dissociate a water in the L-to-M transition, as in the third model (OH[–] transfer model) of Figure 2, that possibly needs concentration of free energy into a water. The motion of a chloride ion toward the cytoplasmic side in

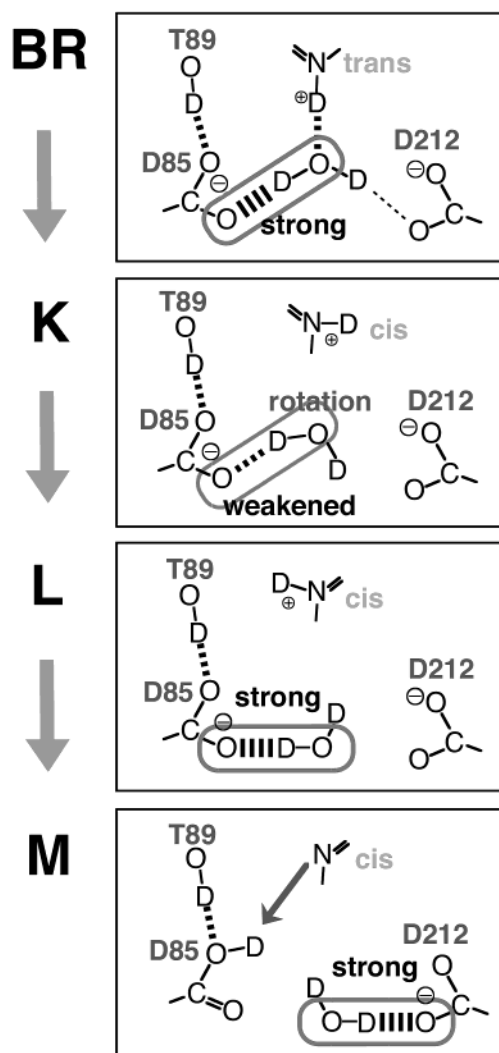


FIGURE 4: Hydration switch model as the proton transfer mechanism from the Schiff base to Asp85. The structure of the Schiff base region in D₂O is schematically drawn. A strong hydrogen bond of water402, whose O–D stretch appears at 2171 cm^{−1}, is highlighted in BR, L, and M. The acceptor is Asp85 in BR and L, while it is switched to Asp212 in M. In this model, hydration switch of water402 from Asp85 to Asp212 is correlated with the proton transfer from the Schiff base to Asp85. The interaction of Thr89 and Asp85 is from our FTIR results (34, 36). The orientation of the N–D group in K is from the theoretical calculation (41), which is consistent with our FTIR results (39). On the other hand, the orientation of the N–D group in L is arbitrary.

halorhodopsin (HR) and the D85T and D85S mutant BR could be explained by the hydration switch model as follows. If the interaction of a chloride with Thr111 in HR (42) (Thr85 or Ser85 in D85T or D85S, respectively) switches to Asp238 (Asp212 in the BR mutants) as the hydration switch model predicts for a water in wild-type BR, electrostatic repulsion between two negative charges possibly makes the chloride binding site unstable. As a consequence, the chloride ion is forced to relocate.

In the hydration switch model, Asp212 plays an important role in the proton transfer from the Schiff base to Asp85. In fact, the D212N mutant exhibits unique properties about the proton pump, which is different from the chloride-pumping mutants of Asp85. D212N pumps a proton at low pH in the presence of chloride, not sulfate (43). In contrast, D212N does not pump a proton at pH > 7, even though a proton donor (the Schiff base) and an acceptor (Asp85) exist (40,

43). In the former case, the hydration switch model suggests that a chloride ion binds close to position 212, and possibly hydrates water402 during the L-to-M transition as Asp212 does in wild-type BR. For the latter case, we previously analyzed the IR data for weakly hydrogen bonded water molecules in D212N, and proposed a model about the proton transfer mechanism on the basis of speculation that there is only one water molecule in the Schiff base region, which has an O–H stretch under very weak hydrogen bonding conditions (2690 cm^{−1} band as the O–D stretch; Figure 3) (20). However, it was then found that the Schiff base region contains more waters as in Figure 1. Through the analysis of strongly hydrogen bonded water, we now reached a model that we call the hydration switch model. Motion of Arg82 is also a notable process, which changes the pK_a of the proton release group (3). Thus, it is likely that each component of an electric quadrupole in the Schiff base region (Figure 1) plays a unique role in the proton transfer from the Schiff base to Asp85. It is noted that the D212N/R82Q mutant protein pumps a proton (44), which needs further explanation. In this particular mutant, a hydration switch may still happen despite a negative charge being absent at position 212. The extremely unstable M state of D212N/R82Q is possibly correlated with this interpretation (44).

Since structures of photointermediates have been reported, it is of interest to compare the distance of a water with the closer carboxyl oxygen in Asp85 or Asp212. According to the L structure by Royant et al. (11), the distance between a water and Asp85 or Asp212 is 2.6 or 2.9 Å, respectively. The recent L structure by Lanyi et al. shows that the distance from water402 to Asp85 or Asp212 is 2.4 or 3.2 Å, respectively (J. K. Lanyi, private communication). These observations imply that the water associates more strongly with Asp85 than with Asp212, as well as in BR (Figures 1 and 4). In contrast, various M structures provided the following values: 3.3 Å with Asp85 and 3.0 Å with Asp212 by Luecke et al. for D96N (12), 2.8 Å with Asp85 and 2.9 Å with Asp212 by Luecke et al. for E204Q (13), 2.8 Å with Asp85 and 2.5 Å with Asp212 by Sass et al. for the wild type (14), 3.1 Å with Asp85 and 3.0 Å with Asp212 by Facciotti et al. for the wild type (15), and 2.4 Å with Asp85 and 2.5 Å with Asp212 by Lanyi and Schobert for the wild type (16). Although it is difficult to determine the distances quantitatively from these structures, the interaction of Asp212 with the water seems to become stronger in M than in L. Thus, the structures of the L and M photointermediates are consistent with the hydration switch model. For a more detailed discussion about the hydrogen bonding strength, the geometrical arrangement of the water and carboxylates also has to be taken into account (45, 46).

These results also suggest the mechanism for water association with Asp96 in the N intermediate. Since there is no counterion around Asp96 upon deprotonation in N, the participation of water molecules to stabilize the negative charge has been suggested (47). We observed that the vibrational character of strongly hydrogen bonded waters is identical among BR, M, and N (Figure 3). This means that there is no strong association of water molecules with the negatively charged Asp96 in N, unlike the case for Asp85 in BR (Figure 1). Helix opening may lead to the uptake of aqueous waters into protein (47–49), whereas the negative charge of Asp96 is stabilized in a manner different from that

of Asp85. How is then the negative charge stabilized at position 96? Several water molecules may stabilize the deprotonated Asp96 in a less organized manner in an open conformation of the cytoplasmic side, whereas limited numbers of water molecules are involved in stabilizing the quadrupole, including Asp85 (Figure 1). Polar residues such as Thr46 may participate in stabilizing the deprotonation state of Asp96.

Spectral acquisition for the X-D stretches also provides information about hydrogen bonds on molecules other than water. By using [^{15}N]Lys-labeled BR, we assigned the N-D stretch of the Schiff base at 2171 and 2123 cm^{-1} to BR and $\sim 2466\text{ cm}^{-1}$ to K (Figure 3a, underlined) (39). Polarized measurements implied that the N-D group points along the membrane after photoisomerization (39). Similar negative bands are observed in the other spectra (Figure 3b-d). By using [^{18}O]Thr-labeled BR, we assigned the O-D stretch of Thr89 at 2506 cm^{-1} to BR and that at $\sim 2466\text{ cm}^{-1}$ to the K, L, and M intermediates (Figure 3a-c) (34, 36). Further analysis by using isotope-labeled BR will lead to a better understanding of the hydrogen bonding alterations during the proton pump in BR.

In conclusion, we describe water structural changes during the photocycle of BR in the whole midinfrared region. Only the K intermediate exhibits frequency changes of the water stretching vibrations that associate with negative charges, indicating that the decay of K involves rehydration of the negative charges by water molecules. We propose a model of proton transfer from the Schiff base to Asp85 being controlled by hydration switch of the bridged water (water402) from Asp85 to Asp212.

ACKNOWLEDGMENT

We thank Prof. Janos K. Lanyi for providing unpublished data about the structure of the L intermediate.

REFERENCES

- Gutman, M., and Nachliel, E. (1997) *Annu. Rev. Phys. Chem.* **48**, 329–356.
- Kandori, H. (2000) *Biochim. Biophys. Acta* **1460**, 177–191.
- Lanyi, J. K. (1998) *J. Struct. Biol.* **124**, 164–178.
- Haupts, U., Tittor, J., and Oesterhelt, D. (1999) *Annu. Rev. Biophys. Biomol. Struct.* **28**, 367–399.
- Luecke, H., Schobert, B., Richter, H.-T., Cartailler, J. P., and Lanyi, J. K. (1999) *J. Mol. Biol.* **291**, 899–911.
- Belrhali, H., Nollert, P., Royant, A., Menzel, C., Rosenbusch, J., Landau, E. M., and Pebay-Peyroula, E. (1999) *Structure* **7**, 909–917.
- Luecke, H. (2000) *Biochim. Biophys. Acta* **1460**, 133–156.
- Sasaki, J., Brown, L. S., Chon, Y.-S., Kandori, H., Maeda, A., Needleman, R., and Lanyi, J. K. (1995) *Science* **269**, 73–75.
- Edman, K., Nollert, P., Royant, A., Belrhali, H., Pebay-Peyroula, E., Hajdu, J., Neutze, R., and Landau, E. M. (1999) *Nature* **401**, 822–826.
- Schobert, B., Cupp-Vickery, J., Hornak, V., Smith, S. O., and Lanyi, J. K. (2002) *J. Mol. Biol.* **321**, 715–726.
- Royant, A., Edman, K., Ursby, T., Pebay-Peyroula, E., Landau, E. M., and Neutze, R. (2000) *Nature* **406**, 645–648.
- Luecke, H., Schobert, B., Richter, H.-T., Cartailler, J. P., and Lanyi, J. K. (1999) *Science* **286**, 255–261.
- Luecke, H., Schobert, B., Cartailler, J.-P., Richter, H.-T., Rosen-garth, A., Needleman, R., and Lanyi, J. K. (2000) *J. Mol. Biol.* **300**, 1237–1255.
- Sass, H. J., Büldt, G., Gessenich, R., Hehn, D., Neff, D., Schlesinger, R., Berendzen, J., and Ormos, P. (2000) *Nature* **406**, 649–653.
- Facciotti, M. T., Rouhani, S., Burkard, F. T., Betancourt, F. M., Downing, K. H., Rose, R. B., McDermott, G., and Glaeser, R. M. (2002) *Biophys. J.* **81**, 3442–3455.
- Lanyi, J. K., and Schobert, B. (2002) *J. Mol. Biol.* **321**, 727–737.
- Maeda, A., Sasaki, J., Shichida, Y., and Yoshizawa, T. (1992) *Biochemistry* **31**, 462–467.
- Maeda, A., Sasaki, J., Yamazaki, Y., Needleman, R., and Lanyi, J. K. (1994) *Biochemistry* **33**, 1713–1717.
- Fischer, W. B., Sonar, S., Marti, T., Khorana, H. G., and Rothschild, K. J. (1994) *Biochemistry* **33**, 12757–12762.
- Kandori, H., Yamazaki, Y., Sasaki, J., Needleman, R., Lanyi, J. K., and Maeda, A. (1995) *J. Am. Chem. Soc.* **117**, 2118–2119.
- Yamazaki, Y., Hatanaka, M., Kandori, H., Sasaki, J., Jan Karstens, W. F., Raap, J., Lugtenburg, J., Bizounok, M., Herzfeld, J., Needleman, R., Lanyi, J. K., and Maeda, A. (1995) *Biochemistry* **34**, 7088–7093.
- Brown, L. S., Sasaki, J., Kandori, H., Maeda, A., Needleman, R., and Lanyi, J. K. (1995) *J. Biol. Chem.* **270**, 27122–27126.
- Yamazaki, Y., Tuzi, S., Saitô, H., Kandori, H., Needleman, R., Lanyi, J. K., and Maeda, A. (1996) *Biochemistry* **35**, 4063–4068.
- Hatanaka, M., Sasaki, J., Kandori, H., Ebrey, T. G., Needleman, R., Lanyi, J. K., and Maeda, A. (1996) *Biochemistry* **35**, 6308–6312.
- Chon, Y.-S., Sasaki, J., Kandori, H., Brown, L. S., Lanyi, J. K., Needleman, R., and Maeda, A. (1996) *Biochemistry* **35**, 14244–14250.
- Hatanaka, M., Kashima, R., Kandori, H., Friedman, N., Sheves, M., Needleman, R., Lanyi, J. K., and Maeda, A. (1997) *Biochemistry* **36**, 5493–5498.
- Hatanaka, M., Kandori, H., and Maeda, A. (1997) *Biophys. J.* **73**, 1001–1006.
- Yamazaki, Y., Kandori, H., Needleman, R., Lanyi, J. K., and Maeda, A. (1998) *Biochemistry* **37**, 1559–1564.
- Maeda, A., Tomson, F. L., Gennis, R. B., Ebrey, T. G., and Balashov, S. P. (1999) *Biochemistry* **38**, 8800–8807.
- Maeda, A., Tomson, F. L., Gennis, R. B., Kandori, H., Ebrey, T. G., and Balashov, S. P. (2000) *Biochemistry* **39**, 10154–10162.
- Kandori, H., Kinoshita, N., Maeda, A., and Shichida, Y. (1998) *J. Phys. Chem. B* **102**, 7899–7905.
- Kandori, H., and Shichida, Y. (2000) *J. Am. Chem. Soc.* **122**, 11745–11746.
- Hayashi, S., and Ohmine, I. (2000) *J. Phys. Chem. B* **104**, 10678–10691.
- Kandori, H., Kinoshita, N., Yamazaki, Y., Maeda, A., Shichida, Y., Needleman, R., Lanyi, J. K., Bizounok, M., Herzfeld, J., Raap, J., and Lugtenburg, J. (1999) *Biochemistry* **38**, 9676–9683.
- Kandori, H., Kinoshita, N., Yamazaki, Y., Maeda, A., Shichida, Y., Needleman, R., Lanyi, J. K., Bizounok, M., Herzfeld, J., Raap, J., and Lugtenburg, J. (2000) *Proc. Natl. Acad. Sci. U.S.A.* **97**, 4643–4648.
- Kandori, H., Yamazaki, Y., Shichida, Y., Raap, J., Lugtenburg, J., Belenky, M., and Herzfeld, J. (2001) *Proc. Natl. Acad. Sci. U.S.A.* **98**, 1571–1576.
- Kandori, H. (1998) *J. Am. Chem. Soc.* **120**, 4546–4547.
- Monosmith, W. B., and Walrafen, G. E. (1984) *J. Chem. Phys.* **15**, 669–674.
- Kandori, H., Belenky, M., and Herzfeld, J. (2002) *Biochemistry* **41**, 6026–6031.
- Needleman, R., Chang, M., Ni, B., Váró, G., Fornés, J., White, S. H., and Lanyi, J. K. (1991) *J. Biol. Chem.* **266**, 11478–11484.
- Hayashi, S., Tajkhorshid, E., and Schulten, K. (2002) *Biophys. J.* **83**, 1281–1297.
- Kolbe, M., Besir, H., Essen, L.-O., and Oesterhelt, D. (2000) *Science* **288**, 1390–1396.
- Moltke, S., Krebs, M. P., Mollaaghababa, R., Khorana, H. G., and Heyn, M. P. (1995) *Biophys. J.* **69**, 2074–2083.
- Brown, L. S., Váró, G., Hatanaka, M., Sasaki, J., Kandori, H., Maeda, A., Friedman, N., Sheves, M., Needleman, R., and Lanyi, J. K. (1995) *Biochemistry* **34**, 12903–12911.
- Gat, Y., and Sheves, M. (1993) *J. Am. Chem. Soc.* **115**, 3772–3773.
- Roussio, I., Friedman, N., Sheves, M., and Ottolenghi, M. (1995) *Biochemistry* **34**, 12059–12065.
- Cao, Y., Váró, G., Chang, M., Ni, B., Needleman, R., and Lanyi, J. K. (1991) *Biochemistry* **30**, 10972–10979.
- Subramaniam, S., Lindahl, M., Bullough, P., Faruqi, A. R., Tittor, J., Oesterhelt, D., Brown, L., Lanyi, J., and Henderson, R. (1999) *J. Mol. Biol.* **287**, 145–161.
- Vonck, J. (2000) *EMBO J.* **19**, 2152–2160.

BI026990D